(12) INTERNATIONAL APPLICATION PUBLISHED UNDER THE PATENT COOPERATION TREATY (PCT)

(19) World Intellectual Property Organization
International Bureau

(43) International Publication Date
22 November 2012 (22.11.2012)

(10) International Publication Number
WO 2012/155195 A1

(51) International Patent Classification:
C01B 25/26 (2006.01) ***H01M 4/12*** (2006.01)
H01M 4/06 (2006.01) ***H01M 6/02*** (2006.01)
H01M 4/38 (2006.01) ***H01M 4/02*** (2006.01)
C01B 25/45 (2006.01) ***H01M 4/36*** (2006.01)

(21) International Application Number: PCT/AU2012/000529

(22) International Filing Date: 11 May 2012 (11.05.2012)

(25) Filing Language: English

(26) Publication Language: English

(30) Priority Data:
2011901842 13 May 2011 (13.05.2011) AU

(71) Applicant *(for all designated States except US)*: **UNIVERSITY OF WOLLONGONG** [AU/AU]; Northfields Avenue, Wollongong, New South Wales 2522 (AU).

(72) Inventor; and
(75) Inventor/Applicant *(for US only)*: **LIU, Hua Kun** [AU/AU]; Northfields Avenue, Wollongong, New South Wales 2522 (AU).

(74) Agents: **CARTER, Christopher John** et al.; Davies Collison Cave, Level 14, 255 Elizabeth Street, Sydney, New South Wales 2000 (AU).

(81) Designated States *(unless otherwise indicated, for every kind of national protection available)*: AE, AG, AL, AM, AO, AT, AU, AZ, BA, BB, BG, BH, BR, BW, BY, BZ, CA, CH, CL, CN, CO, CR, CU, CZ, DE, DK, DM, DO, DZ, EC, EE, EG, ES, FI, GB, GD, GE, GH, GM, GT, HN, HR, HU, ID, IL, IN, IS, JP, KE, KG, KM, KN, KP, KR, KZ, LA, LC, LK, LR, LS, LT, LU, LY, MA, MD, ME, MG, MK, MN, MW, MX, MY, MZ, NA, NG, NI, NO, NZ, OM, PE, PG, PH, PL, PT, QA, RO, RS, RU, RW, SC, SD, SE, SG, SK, SL, SM, ST, SV, SY, TH, TJ, TM, TN, TR, TT, TZ, UA, UG, US, UZ, VC, VN, ZA, ZM, ZW.

(84) Designated States *(unless otherwise indicated, for every kind of regional protection available)*: ARIPO (BW, GH, GM, KE, LR, LS, MW, MZ, NA, RW, SD, SL, SZ, TZ, UG, ZM, ZW), Eurasian (AM, AZ, BY, KG, KZ, RU, TJ, TM), European (AL, AT, BE, BG, CH, CY, CZ, DE, DK, EE, ES, FI, FR, GB, GR, HR, HU, IE, IS, IT, LT, LU, LV, MC, MK, MT, NL, NO, PL, PT, RO, RS, SE, SI, SK, SM, TR), OAPI (BF, BJ, CF, CG, CI, CM, GA, GN, GQ, GW, ML, MR, NE, SN, TD, TG).

Published:
— *with international search report (Art. 21(3))*

(54) Title: LIQUID ASSISTED GRINDING METHOD FOR PRODUCING IMPROVED BATTERY MATERIAL

FIGURE 1

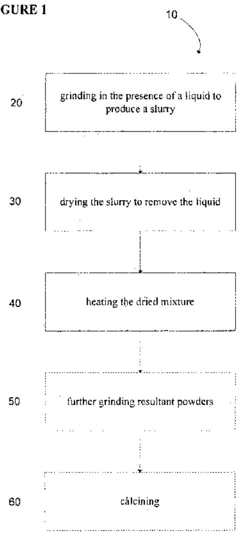

(57) Abstract: A lithium based composite material and method of preparation. Including grinding a mixture of a lithium salt, a metal oxide or salt, a phosphate salt and a carbon source in the presence of a liquid to produce a slurry. The liquid helps the grinding and homogeneous mixing and is not consumed as a reagent. Upon removing the liquid the slurry becomes a dried mixture, and after heating the dried mixture becomes a composite, which can be used as a cathode material in a lithium-ion battery. For example, the composite is $LiFePO_4$-Fe_2P-C and shows a specific capacity of 167 mAh/g at 0.2C and 146 mAh/g at 5C after 100 cycles, respectively. At high current density the example composite exhibits long-term cycling stability, retaining around 96% of its original discharge capacity beyond 1000 cycles, which can meet requirements of a lithium-ion battery for large-scale power applications.

LIQUID ASSISTED GRINDING METHOD FOR PRODUCING IMPROVED BATTERY MATERIAL

Technical Field

[001] The present invention generally relates to advanced electrode materials, such as for use in lithium-ion batteries, and more particularly to a composite material and a method of production or synthesis thereof.

Background

[002] Lithium-ion batteries are currently the dominant power sources for portable electronic devices and are also considered as promising power sources in other areas, such as Electric Vehicles (EV), Hybrid Electric Vehicles (HEV), stationary energy storage for solar and wind electricity generation, as well as smart grids. However, current lithium-ion batteries are approaching limits set by currently used electrode materials. To improve the high energy density, long cycle life, and high-rate capability of lithium-ion battery is a major challenge in next-generation lithium-ion batteries.

[003] For a range of applications, such as EV/HEV, commercial lithium-ion batteries can not yet achieve the desired combination of high energy density, high power, and high rate capability. Apart from the search for new or improved electrode materials with higher specific energy densities, the enhancement of electrode capacity retention at high charge/discharge rates is one of the main challenges in lithium-ion battery research.

[004] Following the pioneering work by Padhi *et al.* (A. K. Padhi, K. S. Nanjundaswamy, J. B. Goodenough, *J. Electrochem. Soc.* **1997**, *144*, 1188), olivine-like $LiFePO_4$ has become known as an attractive electrode material for lithium-ion batteries, for high power applications in particular. This is because of its high theoretical capacity (170 mAh g^{-1}), acceptable operating voltage (3.4 V vs. Li^+/Li), low cost, environmental friendliness, long cycle life, cell safety, and high thermal stability. Nevertheless, a major limitation of previously produced material, which has so far prevented it from being used in large-scale applications, has been its poor high-rate performance, owing to generally low electronic conductivity and low ionic diffusion coefficients. Furthermore, obtaining long term cycling

stability at a high current rate has been a great challenge for this material, as it is necessary for lithium-ion batteries to have long cycle life for EV/HEV commercial applications.

[005] Recently, ultra-fast charging and discharging at very high rates has been reported for $LiFePO_4$ material via creation of an ion conducting lithium phosphate coating on the surface of $LiFePO_4$ nanoparticles. However, the reported long term cycling stability is still not good enough (see B. Kang, G. Ceder, *Nature* 2009, *458*, 190).

[006] Satisfactory long term cycling stability has been achieved through the formation of a mesoporous $LiFePO_4/C$ nanocomposite (118 mAh g^{-1} at 10 C after 1000 cycles) (see G. Wang, H. Liu, J. Liu, S. Qiao, G. M. Lu , P. Munro, H. Ahn, *Adv. Mater.* 2010, *22*, 4944); and by synthesising a $LiFePO_4/C$ composite (~ 85 mAh g^{-1} at 10 C after 2400 cycles) via high-energy ball milling combined with a spray-drying method (see S. J. Kwon, C. W. Kim, W. T. Jeong, K. S. Lee, *J. Power Sources* 2004, *137*, 93). Whilst both of these reported results satisfy the long term cycling stability requirements, the specific discharge capacities are relatively low, and there is much room for further improvement.

[007] There remains a need for new or improved electrode materials and/or a method of producing electrode materials.

[008] The reference in this specification to any prior publication (or information derived from the prior publication), or to any matter which is known, is not, and should not be taken as an acknowledgment or admission or any form of suggestion that the prior publication (or information derived from the prior publication) or known matter forms part of the common general knowledge in the field of endeavour to which this specification relates.

Brief Summary

[009] According to a first broad form, there is provided a composite material and a method of production or synthesis thereof. In one example form, the present invention seeks to provide a lithium based composite material for use in lithium-ion batteries, which improves the performance characteristics of the resultant batteries when used therein. In another example form, the present invention seeks to provide a novel method, which is

relatively simpler than other processing methods and can be used not only to produce lithium based composite cathode materials, such as $LiCoO_2$-C, $LiFeO_2$-C, LiV_3O_8-C, $LiNiO_2$-C, $LiMnPO_4$-C, and $LiCoPO_4$-C), but also to produce metal oxide based composite anode materials, such as Fe_2O_3-C, MnO_2-C, NiO-C, Co_4O_3-C, and V_2O_5-C. These metal oxide composites could also be suitable for other applications.

[010] In an example form, there is provided a method of preparing a lithium based composite material comprising the steps of: grinding a mixture of a lithium salt, a metal oxide or salt, a phosphate salt and a carbon source in the presence of a liquid to produce a slurry, whereby the liquid helps the grinding and homogeneous mixing but is not consumed as a reagent; drying the slurry to remove the liquid to obtain a dried mixture; and, heating the dried mixture to form the lithium based composite material.

[011] In a preferred but non-limiting form, the lithium based composite material is a $LiFePO_4$-Fe_2P-C composite material. Optionally, the lithium salt is lithium carbonate (Li_2CO_3).

[012] In other forms, the lithium salt, metal oxide or salt, or phosphate salt could be selected on the basis of the desired cathode materials (for example $LiCoO_2$-C, $LiFeO_2$-C, LiV_3O_8-C, $LiNiO_2$-C, $LiMnPO_4$-C, and $LiCoPO_4$-C).

[013] Optionally, the metal oxide or salt is iron(II) oxalate dihydrate ($FeC_2O_4.2H_2O$). In other forms, the metal oxide or salt could be selected on the basis of the desired anode materials (for example Fe_2O_3-C, MnO_2-C, NiO-C, and Co_4O_3-C). Optionally, the phosphate salt is ammonium dihydrogen phosphate ($NH_4H_2PO_4$). In a particular example, the carbon source also acts as a reducing agent. Optionally, the carbon source is an organic acid, preferably citric acid ($C_6H_8O_7$).

[014] Preferably, but not necessarily, the lithium salt, the metal oxide or salt, and the phosphate salt are mixed in a stoichiometric molar ratio of about 1:1:1. In a preferred but non-limiting form, the liquid is a ketone, more preferably acetone ($(CH_3)_2CO$).

[015] In a particular example, the liquid helps the homogeneous mixing of the lithium salt, the metal oxide or salt, the phosphate salt and/or the carbon source. In another particular example, the slurry is a suspension or a colloid.

[016] In a preferred but non-limiting form, drying is at a temperature of between about 25 ^{o}C and 100 ^{o}C. Optionally, drying is at a temperature of about 60 ^{o}C. In a preferred but non-limiting form, heating the dried mixture is at a temperature of between about 200 ^{o}C and 600 ^{o}C. Optionally, heating the dried mixture is at a temperature of about 350 ^{o}C.

[017] In a preferred but non-limiting form, heating is performed for between about 1 hour and about 24 hours. Optionally, heating is performed for about 10 hours. In a preferred but non-limiting form, heating is performed in the presence of a noble gas, preferably that is flowing. Optionally, the noble gas is Argon.

[018] In a preferred but non-limiting form, the method also includes the steps of further grinding resultant powders and calcining at a temperature of between about 400 ^{o}C and 800 ^{o}C. Optionally, the calcining is performed at a temperature of about 600 ^{o}C.

[019] In a preferred but non-limiting form, the produced lithium based composite material contains between about 5 wt.% amorphous carbon and about 20 wt.% amorphous carbon. Preferably, but not necessarily, the grinding is performed using a grinding mill such as a mortar and pestle or a wet ball mill. In a preferred but non-limiting form, the lithium based composite material is used as or forms at least part of an electrode in a lithium-ion battery.

[020] In another example form there is provided a lithium based composite material including clusters of olivine phase $LiFePO_4$ in proximity to clusters of Fe_2P, and also including interspersed carbon.

[021] Preferably, the composite material has a capacity of greater than 160 mAh g^{-1}. Preferably, the composite material has a capacity retention of greater than 90 % after 1000 cycles at a rate of 10 C (where 10 C is the numerical value of rated capacity of a cell).

[022] Preferably, the composite material is used as, or forms, at least part of an electrode in a lithium-ion battery.

Brief Description Of Figures

[023] Example embodiments should become apparent from the following description, which is given by way of example only, of at least one preferred but non-limiting embodiment, described in connection with the accompanying figures.

[024] Figure 1 illustrates an example method of preparing a lithium based composite material.

[025] Figure 2 illustrates XRD patterns of example samples: (a) bare-$LiFePO_4$ (0 wt.% C), (b) $LiFePO_4$-Fe_2P-C (1) (5.8 wt.% C), (c) $LiFePO_4$-Fe_2P-C (2) (10.4 wt.% C), and (d) $LiFePO_4$-Fe_2P-C (3) (19.9 wt.% C);

[026] Figure 3 illustrates TGA curves of bare-$LiFePO_4$ and $LiFePO_4$-Fe_2P-C example composite powders estimated to contain (1) 5.8 wt.% C, (2) 10.4 wt.% C, and (3) 19.9 wt.% C;

[027] Figure 4 illustrates secondary electron FESEM micrographs of (a) bare-$LiFePO_4$, (b) $LiFePO_4$-Fe_2P-C (1) (5.8 wt.% C), (c) $LiFePO_4$-Fe_2P-C (2) (10.4 wt.% C), and (d) $LiFePO_4$-Fe_2P-C (3) (19.9 wt.% C);

[028] Figure 5 illustrates high contrast backscattered FESEM micrographs of (a) bare-$LiFePO_4$, (b) $LiFePO_4$-Fe_2P-C (1) (5.8 wt.% C), (c) $LiFePO_4$-Fe_2P-C (2) (10.4 wt.% C), and (d) $LiFePO_4$-Fe_2P-C (3) (19.9 wt.% C);

[029] Figure 6 illustrates EDS spectra of particles in an example $LiFePO_4$-Fe_2P-C composite: (a) $LiFePO_4$/C particle, with high contrast, backscattered FESEM image of source particle in the inset; (b) Fe_2P/C particle, with arrow indicating source particle in (a) inset;

[030] Figure 7 illustrates example magnetic hysteresis loops measured at 5 K between ±10000 Oe after field cooling in 500 Oe;

[031] Figure 8 illustrates short-term cycle life performance (a); long-term cycle life performance beyond 1000 cycles at 10 C for an example $LiFePO_4$-Fe_2P-C (1) electrode (b); the 100th cycle galvanostatic charge-discharge profiles at different current densities from 0.2 to 10 C between 4.3 and 2.5 V for an example $LiFePO_4$-Fe_2P-C (1) electrode (c); cyclic voltammogram of an example $LiFePO_4$-Fe_2P-C (1) electrode at a scan rate of 0.1 mV/s (d); EIS spectra of bare-$LiFePO_4$ and example $LiFePO_4$-Fe_2P-C electrodes, and the equivalent circuit (inset) used to fit the impedance data (e);

[032] Figure 9 illustrates high contrast back-scattered FESEM images of (a) $LiFePO_4$-Fe_2P-C (1) (5.8 wt.% C), (b) $LiFePO_4$-Fe_2P-C (2) (10.4 wt.% C), and (c) $LiFePO_4$-Fe_2P-C (3) (19.9 wt.% C) example composite powders. It can be observed that the sample shown in (a) with 5.8 wt.% C ($LiFePO_4$-Fe_2P-C (1)) exhibits a higher fraction of $LiFePO_4$/Fe_2P interface coupling and highly porous conductive architecture among the particles, as compared to the other two samples;

[033] Figure 10 illustrates TEM and HRTEM images obtained from (a) bare-$LiFePO_4$ and (b)-(f) $LiFePO_4$-Fe_2P-C (1) (5.8 wt.% C) composite: (c)-(e) study of a region containing $LiFePO_4$ surrounded by a 3 nm carbon-rich layer, marked C, (f) HRTEM image of separate $LiFePO_4$ crystal surrounded by carbon-rich layer marked C. Inset is a fast Fourier transform of the image, and the orientation is close to (212).

Preferred Embodiments

[034] The following modes, given by way of example only, are described in order to provide a more precise understanding of the subject matter of a preferred embodiment or embodiments.

[035] The Applicant has identified a relatively simple and fast liquid assisted grinding method to ensure intimate and homogeneous mixing of elements or compounds approaching an atomic or molecular level. The grinding action can be applied by a grinder, such as a variety of grinding mills, being a machine or apparatus for producing fine

particle size reduction, typically through attrition and compressive forces at the grain size level. For example, a mortar and pestle or similar apparatus that applies pressure to the components being mixed. Another suitable example includes wet-ball milling, using suitable milling balls providing an appropriate grinding mechanism.

[036] The liquid assisted grinding process is combined with a solid state reaction to synthesize a composite material, in one embodiment having application as an electrode material for use in a battery, for example a $LiFePO_4$-Fe_2P-C composite produced with a porous conductive structure. A range of other example resultant lithium based materials can be produced using the liquid assisted grinding process. For example lithium based composite materials such as: $LiCoO_2$-C, $LiFeO_2$-C, LiV_3O_8-C, $LiNiO_2$-C, $LiMnPO_4$-C, and $LiCoPO_4$-C. Other metal oxide based composite materials could also be produced such as Fe_2O_3-C, MnO_2-C, NiO-C, Co_4O_3-C, and V_2O_5-C, etc..

[037] Other $LiFePO_4$ materials made by known direct solid state reactions do not show high rate capability, or as good high-rate long-term cycling performance as the example $LiFePO_4$-Fe_2P-C composite material, when used as an electrode, as produced by the present methods. In one example, electrochemical measurements demonstrate that the synthesised example $LiFePO_4$-Fe_2P-C composite delivers a high capacity of 167 mAh g-1 at 0.2C at 100th cycle and displays long term cycling stability with capacity retention of around 96 % (131 mAh g-1) even after 1000 cycles at 10 C.

[038] Industrial scale grinding and mixing apparatus could be effectively used to achieve similar or better results. For example, a paddle blender is designed for uniformly wet and dry mixing and blending and provides a good environment for initially mixing a wide distribution of particle size and bulk densities without segregation of powders. A paddle blender or similar type of mixing apparatus could be effective for an initial stage of homogenised mixing. A liquid assisted grinding stage could then be applied, for example using wet-ball milling. This process can be used to produce a variety of composite materials for use in batteries, such as lithium-ion batteries, with improved characteristics.

[039] Referring to **Fig. 1**, there is provided a method 10 of preparing a lithium based composite material. Method 10 includes step 20 of grinding a mixture of a lithium salt, a

metal oxide or salt, a phosphate salt and a carbon source in the presence of a liquid to produce a slurry. Importantly, the liquid is not consumed as a reagent in a chemical reaction (i.e. the liquid is non-reactive, it acts as a reaction aid for other components). Instead the liquid acts as a facilitating agent for improved physical mixing and/or grinding. At step 30 the slurry is dried to remove (e.g. evaporate) the liquid so as to obtain a dried mixture. At step 40 the dried mixture is heated, preferably calcined, to decompose or otherwise react the lithium salt, the metal oxide or salt, the phosphate salt and the carbon source to chemically produce the new lithium based compound.

[040] Various advantages are obtained from this method, including for example: a much shorter time-frame than is normally required for high energy ball milling (which is typically 2-3 days); a lower energy consumption compared to high energy ball milling; advantageous magnetic phases result in the lithium based composite material; the process can be performed at relatively low temperature.

[041] In a preferred example, the lithium based composite material is a $LiFePO_4$-Fe_2P-C composite material. The lithium salt can be lithium carbonate (Li_2CO_3). In other forms, the lithium salt, metal oxide or salt, or phosphate salt could be selected on the basis of the desired cathode materials (for example $LiCoO_2$-C,. $LiFeO_2$-C, LiV_3O_8-C, $LiNiO_2$-C, $LiMnPO_4$-C, and $LiCoPO_4$-C). The metal oxide or salt can be iron(II) oxalate dihydrate ($FeC_2O_4.2H_2O$). In other forms, the metal oxide or salt could be selected on the basis of the desired anode materials (for example Fe_2O_3-C, MnO_2-C, NiO-C, and Co_4O_3-C). The phosphate salt can be ammonium dihydrogen phosphate ($NH_4H_2PO_4$). In a particular example, the carbon source also acts as a reducing agent. The carbon source can be an organic compound, for example citric acid ($C_6H_8O_7$).

[042] The lithium salt, the metal oxide or salt and the phosphate salt are preferably mixed in a stoichiometric molar ratio of about 1:1:1. The liquid is preferably a ketone, such as acetone. The liquid can help the homogeneous mixing. The slurry could be a suspension or a finer submicron colloid.

[043] Drying step 30 is preferably performed at a temperature of between about 25 °C and 100 °C. Most preferably drying is performed at a temperature of about 60 °C. Heating

step 40 of the dried mixture is preferably performed at a temperature of between about 200 °C and 600 °C. Most preferably, heating the dried mixture is at a temperature of about 350 °C. Heating is preferably performed for between about 1 hour and about 24 hours, most preferably the heating is performed for about 10 hours. Also preferably, heating is performed in the presence of a noble gas, such as Argon, and the gas is a flow of gas.

[044] Method 10 may also included additional step 50 of further grinding the resultant dried and heated powders, as well as additional step 60 of calcining, for example at a temperature of between about 400 °C and 800 °C. Optionally, the calcining step 60 can be performed at a temperature of about 600 °C.

[045] The produced lithium based composite material may contain various levels of carbon. In the experiments performed by the Applicant, varying the citric acid volume produced between about 5 wt.% amorphous carbon and about 20 wt.% amorphous carbon in the produced $LiFePO_4$-Fe_2P-C composite material.

[046] Grinding can be performed using a variety of grinders, grinding apparatus or grinding mills, such as simple mortar and pestle or a wet ball mill. The produced lithium based composite material can be used as part of an electrode in a lithium-ion battery. The $LiFePO_4$-Fe_2P-C composite material includes clusters of antiferromagnetic olivine phase $LiFePO_4$ in proximity to clusters of ferromagnetic Fe_2P, and also includes interspersed carbon. The composite material was found to have a capacity of greater than 160 mAh g^{-1}, and a capacity retention of greater than 90 % after 1000 cycles at a rate of 10 C.

<u>$LiFePO_4$-Fe_2P-C composite material</u>

[047] The following example provides a more detailed discussion of a particular embodiment. The example is intended to be merely illustrative and not limiting to the scope of the present invention.

[048] A simple ultra-fast liquid assisted grinding method, combined with a solid state reaction, has been developed to synthesize a $LiFePO_4$-Fe_2P-C composite having a porous conductive architecture. Lithium carbonate (Li_2CO_3), iron(II) oxalate dihydrate ($FeC_2O_4.2H_2O$), and ammonium dihydrogen phosphate ($NH_4H_2PO_4$) in a stoichiometric

molar ratio of about 1:1:1 were used as starting materials, and citric acid ($C_6H_8O_7$) was used as a reducing agent and a carbon source.

[049] The precursor reactants were ground thoroughly, and a slurry was made with liquid acetone using mortar and pestle, which provided an unexpected degree of intimate and homogeneous mixing. The slurry was then dried in an oven at about 60 °C to remove acetone from the slurry. To decompose and react the carbonate, oxalate, and phosphate, the dried mixture was placed in a tube furnace and heat treated at about 350 °C for about 10 hours under flowing argon. The resultant powders were cooled to room temperature and thoroughly reground. The powders were then again calcined at about 600 °C for about 10 hours under flowing argon. For comparison, bare-$LiFePO_4$ and $LiFePO_4$-Fe_2P-C composites containing 5.8 wt.% C [$LiFePO_4$-Fe_2P-C (1)], 10.4 wt.% C [$LiFePO_4$-Fe_2P-C (2)], and 19.9 wt.% C [$LiFePO_4$-Fe_2P-C (3)] were obtained by using different amounts of citric acid.

[050] To form an electrode and to test the electrochemical performance, powder samples were mixed with acetylene black (AB) and a binder, polyvinylidene fluoride, in a weight ratio of 80:15:5 in a solvent, *N*-methyl-2-pyrrolidone (anhydrous, 99.5 %). The slurry was uniformly spread onto aluminium foil substrates with an area of 1 cm^2. The coated electrodes were dried in a vacuum oven at 100 °C for 24 h and then pressed. CR 2032 coin-type cells were assembled in an Ar-filled glove box. The electrochemical coin cells contained the coated materials on aluminium foil as the working electrode, lithium foil as counter electrode and reference electrode, porous polypropylene as the separator, and 1 M $LiPF_6$ in a 50:50 (v/v) mixture of ethylene carbonate and dimethyl carbonate as the electrolyte. The cells were galvanostatically charged and discharged in the range of 4.3-2.5 V at different rates of 0.2-10 C using a computer-controlled charger system. Cyclic voltammetry (with a scan rate of 0.1 mVs^{-1} between 4.3 and 2.5 V (versus Li/Li^+)) and electrochemical impedance spectroscopy (EIS) were performed on the electrodes. The AC amplitude was 5 mV, and the frequency range applied was 100 kHz - 0.01 Hz.

Analysis

[051] $LiFePO_4$-Fe_2P-C composites with a porous conductive architecture were created, which include distinct regions or clusters containing antiferromagnetic (AFM) $LiFePO_4$ in

close proximity to ferromagnetic (FM) Fe_2P. The microstructure was achieved by using the liquid assisted solid state reaction method, which is different from all known methods reported in the literature. An AFM/FM "exchange bias" (EB) effect is believed to occur, as evidenced by a particular type of shifting of the magnetic hysteresis loops. The Applicant attributes this to the occurrence of $LiFePO_4/Fe_2P$ interface coupling.

[052] Based on the Applicant's results the electrochemical performance of $LiFePO_4$-Fe_2P-C composite cathodes is unexpectedly enhanced by increasing the volume fraction of fine distributions of $LiFePO_4/Fe_2P$ due to the liquid-assisted method used.

[053] Electrochemical measurements demonstrate that the synthesised $LiFePO_4$-Fe_2P-C composite delivers a high capacity of about 167 mAh g^{-1} at 0.2 C at the 100th cycle and displays long term cycling stability with a capacity retention of around 96 % (about 131 mAh g^{-1}), even after 1000 cycles at 10 C.

[054] X-ray diffraction (XRD) results from the obtained samples are shown in **Fig. 2**. The profiles of the diffraction peaks can be indexed according to the olivine $LiFePO_4$ phase (JCDPS Card Number 40-1499). Any broad peaks or lines corresponding to amorphous or crystalline carbon were of insufficient intensity to be detected against the background in the XRD pattern of the $LiFePO_4$-Fe_2P-C composites. XRD patterns obtained from the carbon coated samples indicate that iron phosphide phase (barringerite Fe_2P, peak at $2\theta = 40.28^o$) begins to form during the annealing process. XRD pattern from bare-$LiFePO_4$ has not provided evidence of Fe_2P peaks. It is therefore possible that carbon originating from the citrate framework has acted as a reductant under the Argon atmosphere during the annealing process.

[055] To estimate the amount of amorphous carbon in the $LiFePO_4$-Fe_2P-C composites, TGA was carried out in air (see **Fig. 3**). The samples were heated from 50 to 1000 °C at a rate of 5 °C/min. As can be seen from **Fig. 3**, bare-$LiFePO_4$ and $LiFePO_4$-Fe_2P-C powders started to oxidize slowly in air at temperatures above 365 °C, with rapid oxidation above 450 °C. The retained mass of the bare-$LiFePO_4$ powder was increased by 4.8 wt.%, which could be attributed to the oxidation of Fe(II) to Fe(III). Meanwhile, the $LiFePO_4$-Fe_2P-C composite powders showed rapid mass loss between 400-700 °C, which corresponds to the

burning of carbon. The difference in weight between bare-$LiFePO_4$ and $LiFePO_4$-Fe_2P-C powders after the oxidation could be translated into the amount of amorphous carbon in the composites. With the use of this method, it was estimated that the amount of amorphous carbon in the composites were approximately 5.8 wt.% C [$LiFePO_4$-Fe_2P-C (1)], 10.4 wt.% C [$LiFePO_4$-Fe_2P-C (2)], and 19.9 wt.% C [$LiFePO_4$-Fe_2P-C (3)], as obtained from different amounts of citric acid used. The specific surface areas of the synthesised products were also measured by the 15 points Brunauer-Emmett-Teller (BET) N_2 adsorption method. The $LiFePO_4$-Fe_2P-C (1) composite containing 5.8 wt% C shows the highest specific surface area (33.14 m^2g^{-1}), while bare-$LiFePO_4$, $LiFePO_4$-Fe_2P-C (2) (10.4 wt.%C), and $LiFePO_4$-Fe_2P-C (3) (19.9 wt.%C) have specific surface areas of 1.17, 16.74, and 14.25 m^2g^{-1}, respectively.

[056] Secondary electron field emission scanning electron microscopy (FESEM) images of the bare-$LiFePO_4$ and $LiFePO_4$-Fe_2P-C composites with different carbon contents are shown in **Fig. 4.** It was observed that the growth of the $LiFePO_4$ grains is inhibited by the carbon and Fe_2P that are formed during the heat treatment process. In **Fig. 4(b-d)**, the FESEM images indicate more abrupt particle growth with increasing carbon content in the sample, which may be caused by the agglomeration of excess carbon in the sample where Fe_2P nanoclusters are being trapped. The porous network structure, along with small particles and rough surfaces, can be clearly observed in **Fig. 4(b)**. As shown in **Fig. 4(c, d)**, it is obvious that with increasing carbon content, the porous network structure with rough surfaces gradually disappears, while agglomerated larger particles with smooth surfaces appear.

[057] FESEM high-contrast backscattered imaging (see **Fig. 5**) of the obtained powders was performed with qualitative calibration of the three most distinct phases (Fe_2P, $LiFePO_4$, and C) that are present in local regions of constant grey level. This was achieved by using energy dispersive spectroscopy (EDS) spot analysis performed on regions of constant grey level (see **Fig. 6**). The light grey regions in the FESEM image are composed of $LiFePO_4$ particles with amorphous carbon (see **Fig. 6(a)**), whereas the greyish white regions represent Fe_2P particles with amorphous carbon (see **Fig. 6(b)**). Examination of **Fig. 5(b-d)** reveals the presence of inhomogeneous distributions of nanoscale Fe_2P particles (white), in a highly porous architecture of $LiFePO_4$ (light grey) and carbon (dark

grey). Despite the inhomogeneous nature of the microstructures, it was observed that the $LiFePO_4$-Fe_2P-C composite containing 5.8 wt.% C (see **Fig. 5(b)**) exhibited the largest fraction of local areas with a fine distribution of Fe_2P particles in close contact with $LiFePO_4$ and carbon (compare **Fig. 5(b)** with **Fig. 5(c)** and **Fig. 5(d)**). It was also observed that this sample (5.8 wt.% C) had a particularly porous conductive architecture (see **Fig. 9**). These observations are consistent with the formation of a higher fraction of $LiFePO_4/Fe_2P$ interface coupling, with implications for magnetic properties. With increasing carbon content, the Fe_2P particles become connected with the primary particles of $LiFePO_4$ and also become denser. This is caused by the agglomeration of the excess carbon in the sample where Fe_2P particles are being trapped (see **Fig. 5(d)**).

[058] Preliminary magnetic measurements revealed additional information which can be associated with structural evolution in the samples. The exchange interaction at the interface between a ferromagnetic (FM) and antiferromagnetic (AFM) component often results in an interesting phenomenon called "exchange bias" (EB), which is manifested by a shift in the hysteresis loop along the field axis when the system is cooled down in an external magnetic field. However, so far, there has been no experimental determination of an exchange bias (EB) effect in $LiFePO_4/Fe_2P$ interface coupling in $LiFePO_4$ materials, even though the magnetic structure and properties of $LiFePO_4$ have been re-examined theoretically and experimentally. Compared to the other samples investigated, a large shift was observed in the magnetic hysteresis loop for the sample containing 5.8 wt% C. Assuming that this shift is associated with an exchange bias effect, the magnitude of this shift in the field axis can be defined as the EB (exchange bias) field, $-H_E = (H_1 + H_2)/2$, where H_1 and H_2 are the left and right coercive fields, respectively. Results for different samples are shown in **Fig. 7**. The maximum value of H_E is 634 Oe with a 500 Oe cooling field for the 5.8 wt% C containing sample, which is larger than the value for the other samples at 5 K. Comparison of the EB effect among the samples indicates that the effect is stronger for the 5.8 wt% C containing sample and is in descending order of $LiFePO_4$-Fe_2P-C (1) > $LiFePO_4$-Fe_2P-C (2) > $LiFePO_4$-Fe_2P-C (3). This trend is coincident with the observation that the fraction of local areas containing a fine distribution of Fe_2P particles in close contact with $LiFePO_4$ also decreases in the same way, where the largest fraction is observed in the sample containing 5.8 wt% C. The same trend was also observed for surface area measurements, with BET surface areas of 33.14, 16.74, 14.25, and 1.17 m^2g^{-1}

for the 5.8, 10.4, and 19.9 wt.% C containing samples and bare-$LiFePO_4$, respectively, and in electrochemical impedance spectroscopy (EIS) analysis.

[059] The electrochemical performances of the prepared samples were evaluated systematically using CR2032 coin cells (see **Fig. 8**). The short-term cycle life performances of the bare-$LiFePO_4$ and $LiFePO_4$-Fe_2P-C composite electrodes at 10 C charge/discharge rates are shown in **Fig. 8(a)**. The initial discharge capacities were measured to be 43, 59, 89, and 137 mAh g^{-1} with a capacity retention of 40, 56, 84, and 136 mAh g^{-1} at the 120th cycle at the 10 C rate for the bare-$LiFePO_4$, $LiFePO_4$-Fe_2P-C (3), $LiFePO_4$-Fe_2P-C (2), and $LiFePO_4$-Fe_2P-C (1) electrodes, respectively. The electrochemical performance among the carbon coated samples is in descending order of $LiFePO_4$-Fe_2P-C (1) > $LiFePO_4$-Fe_2P-C (2) > $LiFePO_4$-Fe_2P-C (3). The electrode composed of $LiFePO_4$-Fe_2P-C (1) (5.8 wt.% C) shows the best electrochemical performance, even at the high current density of 10 C.

[060] In order to fully estimate the electrochemical performance of the $LiFePO_4$-Fe_2P-C (1) (5.8 wt.% C) composite electrode, the cycling behaviours at different current densities of 0.2, 2, 5 and 10 C were measured at the 100th cycle, and their corresponding charge-discharge voltage profiles are shown in **Fig. 8(c)**. The $LiFePO_4$-Fe_2P-C (1) (5.8wt.% C) composite electrode shows long and flat voltage plateaus in the 3.4 - 3.5 V range, and the small voltage difference between the charge-discharge plateaus indicates its good kinetics. This observation is also supported by the cyclic voltammogram (CV curve) shown in **Fig. 8(d)**. The well defined sharp redox peaks in the range of 3.26 - 3.70 V can be attributed to the Fe^{2+}/Fe^{3+} redox couple reaction, corresponding to lithium extraction and insertion in the $LiFePO_4$ crystal structure. The 100th cycle discharge capacities were measured to be 167 mAh g^{-1} at 0.2 C, 159 mAh g^{-1} at 2 C, 146 mAh g^{-1} at 5 C, and 136 mAh g^{-1} at 10 C for the $LiFePO_4$-Fe_2P-C (1) (5.8 wt.%C) electrode, respectively. At the low current density of 0.2 C (5 hours charge and 5 hours discharge), the discharge capacity (167 mAh g^{-1}) is very close to the theoretical capacity of $LiFePO_4$ (170 mAh g^{-1}). Even at the high current rate of 10 C (6 minutes for charging and 6 minutes for discharging), a capacity of 136 mAh g^{-1} is still obtained, demonstrating that the $LiFePO_4$-Fe_2P-C (1) (5.8 wt.% C) composite can tolerate high rate charge and discharge. The capacity fading observed is only about 18 % with an increasing charge-discharge rate from 0.2 to 10 C.

[061] The composite electrode was life tested at a high current density of 1700 mA g^{-1} (10 C rate) for long term cycling, as batteries are required to operate at high current density and to have a cycle life of more than 2000 cycles for EV/HEV applications. Therefore, the $LiFePO_4$-Fe_2P-C (1) (5.8 wt.% C) electrode was cycled at the 10 C rate (6 minutes for charging and 6 minutes for discharging) for 1000 cycles (see **Fig. 8(b)**).

[062] Surprisingly, the $LiFePO_4$-Fe_2P-C (1) (5.8 wt.% C) electrode exhibited superior electrochemical performance, with a capacity retention of around 96 % (131 mAh g^{-1}) of its original discharge capacity after 1000 cycles at the high current rate of 10 C. Such outstanding electrochemical performance can meet the demands of many high power applications.

[063] However, to understand the effect of $LiFePO_4/Fe_2P$ interface coupling along with that of the carbon coating on the charge transfer resistance of electrodes, AC impedance measurements were carried out at room temperature (see **Fig. 8(e)**). The impedance curves show one compressed semicircle in the medium-frequency region, which could be assigned to the charge-transfer resistance (R_{ct}). The spike or inclined line at the low frequency end indicates the Warburg impedance (W) of long-range lithium-ion diffusion. The charge transfer resistance (R_{ct}) was calculated to be 148 Ω cm^{-2} for the bare-$LiFePO_4$, 28 Ω cm^{-2} for the $LiFePO_4$-Fe_2P-C (1), 37 Ω cm^{-2} for the $LiFePO_4$-Fe_2P-C (2), and 60 Ω cm^{-2} for the $LiFePO_4$-Fe_2P-C (3) electrodes, respectively. Basically, a higher carbon content sample shows lower charge transfer resistance (R_{ct}), and generally, this trend is also logical. Under this consideration, the R_{ct} should be in order of $LiFePO_4$-Fe_2P-C (3) (19.9 wt.% C) < $LiFePO_4$-Fe_2P-C (2) (10.4 wt.% C) < $LiFePO_4$-Fe_2P-C (1) (5.8 wt.% C), but the reality is the inverse, since $LiFePO_4$-Fe_2P-C (1) < $LiFePO_4$-Fe_2P-C (2) < $LiFePO_4$-Fe_2P-C (3). At this point, the Applicant contends that this R_{ct} is not only influenced by the carbon content, but also strongly influenced by the interface coupling of $LiFePO_4/Fe_2P$ clusters.

[064] The $LiFePO_4$-Fe_2P-C (1) sample exhibits more and stronger interface coupling of antiferromagnetic (AFM) and ferromagnetic (FM) clusters than the other samples, which increases the effective interface areas, facilitates more rapid charge transfer, and reduces

the charge transfer resistance, leading to the huge shift in the magnetic hysteresis loop. So, the excellent electrochemical performance of the $LiFePO_4$-Fe_2P-C (1) (5.8 wt.% C) composite could be attributed to the porous conductive architecture with large and strong interface coupling of $LiFePO_4/Fe_2P$, which increases the contact area among the carbon, Fe_2P clusters, and $LiFePO_4$ particles, providing multidimensional channels for charge transfer and reducing the resistance for lithium ion migration. Moreover, the composite with porous architecture can ‘suck up’ electrolyte to enormously shorten the diffusive distance of lithium ions.

[065] Transmission electron microscopy (TEM) was used to investigate the morphology and structure of the bare sample and $LiFePO_4$-Fe_2P-C (1) (5.8 wt.% C) composite. It was clearly observed that the crystallite size of this composite is much smaller than that of the bare $LiFePO_4$. The set of images in **Fig. 10(c)-(e)** shows a $LiFePO_4$ particle at increasing magnification. The particle (bottom right of **Fig. 10(c)**) is located over a hole in the holey carbon support film and is surrounded by a layer of carbon about 2-3 nm thick, marked C in **Fig. 10(d)** and **Fig. 10(e)**. The high resolution TEM (HRTEM) image (**Fig. 10(e)**) revealed lattice plane contrast consistent with (020) $LiFePO_4$ ($d_{020} = 0.51$ nm) and contrast around the edge of the particle consistent with amorphous carbon. HRTEM imaging of other regions containing single $LiFePO_4$ particles revealed similar contrast associated with the presence of a layer of amorphous carbon around the edges of the particles (marked C in **Fig. 10(f)**), a result consistent with a real carbon-rich reaction product, rather than, for example, a contamination build-up during electron microscope examination. In the case of **Fig. 10(f)**, the lattice image and associated fast Fourier transform (inset, **Fig. 10(f)**) are consistent with a single $LiFePO_4$ crystal with orientation close to (212).

[066] It has been demonstrated that the fabrication of lithium based composites with strong and extensive antiferromagnetic (AFM) and ferromagnetic (FM) interface coupling of $LiFePO_4/Fe_2P$ provide a versatile and general means for improving the electrochemical properties of materials, such as $LiFePO_4$ materials, and also demonstrates a new exchange bias phenomenon and its ability to enhance the electrochemical performance of lithium-ion battery electrodes.

[067] Optional embodiments of the present invention may also be said to broadly consist in the parts, elements and features referred to or indicated herein, individually or collectively, in any or all combinations of two or more of the parts, elements or features, and wherein specific integers are mentioned herein which have known equivalents in the art to which the invention relates, such known equivalents are deemed to be incorporated herein as if individually set forth.

[068] Although a preferred embodiment has been described in detail, it should be understood that various changes, substitutions, and alterations can be made by one of ordinary skill in the art without departing from the scope of the present invention.

The claims:

1. A method of preparing a lithium based composite material comprising the steps of:

grinding a mixture of a lithium salt, a metal oxide or salt, a phosphate salt and a carbon source in the presence of a liquid to produce a slurry, whereby the liquid helps the grinding and homogeneous mixing but is not consumed as a reagent;

drying the slurry to remove the liquid to obtain a dried mixture; and,

heating the dried mixture to form the lithium based composite material.

2. The method of claim 1, wherein the lithium based composite material is a $LiFePO_4$-Fe_2P-C composite material.

3. The method of either claim 1 or 2, wherein the lithium salt is lithium carbonate (Li_2CO_3).

4. The method of any one of claims 1 to 3, wherein the lithium salt, the metal oxide or salt, or the phosphate salt is selected on the basis of desired cathode materials.

5. The method of any one of claims 1 to 4, wherein the metal oxide or salt is iron(II) oxalate dihydrate ($FeC_2O_4.2H_2O$).

6. The method of any one of claims 1 to 4, wherein the metal oxide or salt is selected on the basis of desired anode materials.

7. The method of any one of claims 1 to 6, wherein the phosphate salt is ammonium dihydrogen phosphate ($NH_4H_2PO_4$).

8. The method of any one of claims 1 to 7, wherein the carbon source also acts as a reducing agent.

9. The method of any one of claims 1 to 8, wherein the carbon source is an organic acid.

10. The method of claim 9, wherein the organic acid is citric acid ($C_6H_8O_7$).

11. The method of any one of claims 1 to 10, wherein the lithium salt, the metal oxide or salt, and the phosphate salt are mixed in a stoichiometric molar ratio of about 1:1:1.

12. The method of any one of claims 1 to 11, wherein the liquid is a ketone.

13. The method of any one of claims 1 to 12, wherein the liquid is acetone ($(CH_3)_2CO$).

14. The method of any one of claims 1 to 13, wherein the liquid partially dissolves the lithium salt, the metal oxide or salt, the phosphate salt or the carbon source.

15. The method of any one of claims 1 to 14, wherein the slurry is a suspension or a colloid.

16. The method of any one of claims 1 to 15, wherein the drying is at a temperature of between about 25 °C and 100 °C.

17. The method of any one of claims 1 to 16, wherein the drying is at a temperature of about 60 °C.

18. The method of any one of claims 1 to 17, wherein the heating of the dried mixture is at a temperature of between about 200 °C and 600 °C.

19. The method of any one of claims 1 to 18, wherein the heating of the dried mixture is at a temperature of about 350 °C.

20. The method of any one of claims 1 to 19, wherein the heating is performed for between about 1 hour and about 24 hours.

21. The method of any one of claims 1 to 20, wherein the heating is performed for about 10 hours.

22. The method of any one of claims 1 to 21, wherein the heating is performed in the presence of a noble gas.

23. The method of claim 22, wherein the noble gas is Argon.

24. The method of any one of claims 1 to 23, additionally including the steps of further grinding a resultant powder and calcining at a temperature of between about 400 °C and about 800 °C.

25. The method of claim 24, wherein the calcining is performed at a temperature of about 600 °C.

26. The method of any one of claims 1 to 25, wherein the lithium based composite material contains between about 5 wt.% amorphous carbon and about 20 wt.% amorphous carbon.

27. The method of any one of claims 1 to 26, wherein the grinding is performed using a grinder or a grinding mill.

28. The method of any one of claims 1 to 27, wherein the lithium based composite material is used as at least part of an electrode in a lithium-ion battery.

29. A lithium based composite material including clusters of olivine phase $LiFePO_4$ in proximity to clusters of Fe_2P, and also including interspersed carbon.

30. The lithium based composite material of claim 29, wherein the composite material has a capacity of greater than 160 mAh g^{-1}.

31. The lithium based composite material of either claim 29 or 30, wherein the composite material has a capacity retention of greater than 90 % after 1000 cycles at a rate of 10 C.

32. The lithium based composite material of any one of claims 29 to 31, wherein the composite material forms at least part of an electrode in a lithium-ion battery.

FIGURE 1

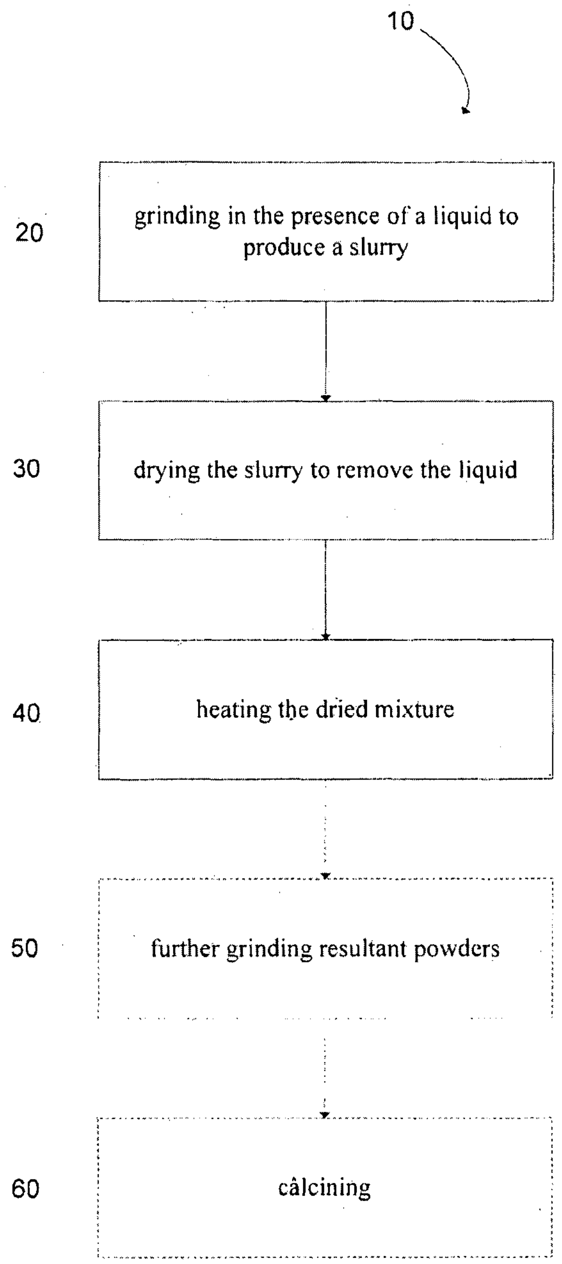
10
20
grinding in the presence of a liquid to produce a slurry
30
drying the slurry to remove the liquid
40
heating the dried mixture
50
further grinding resultant powders
60
calcining

FIGURE 2

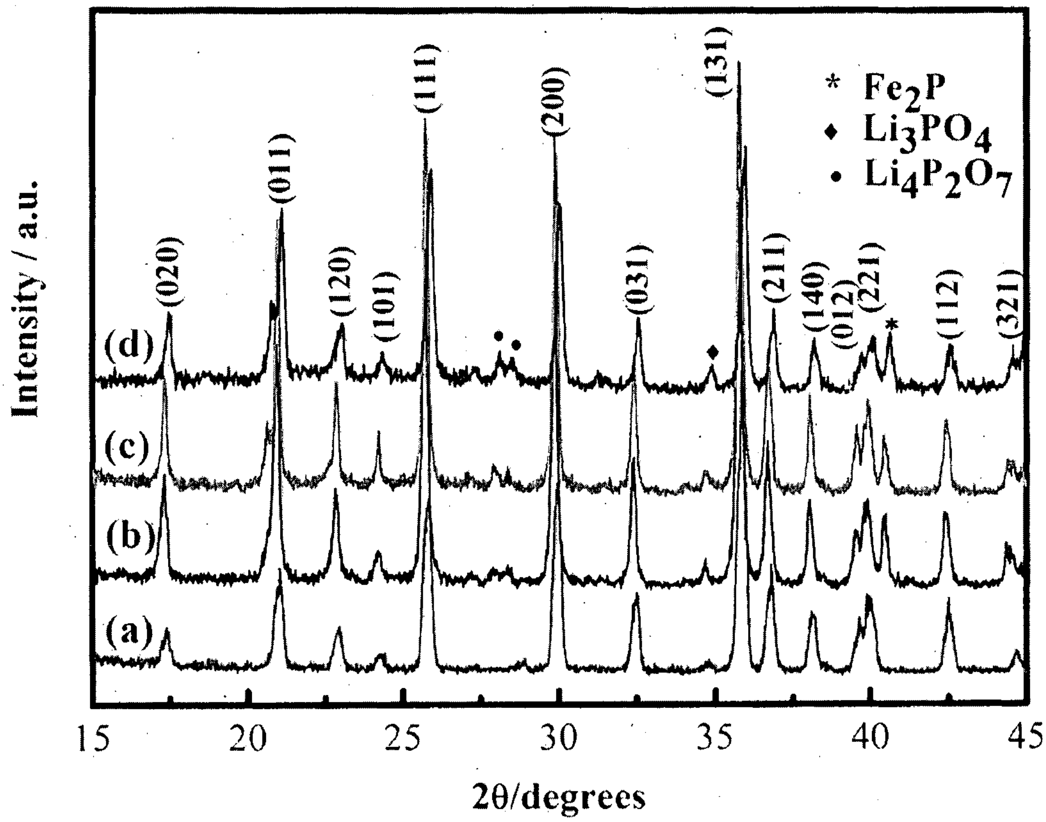
Intensity / a.u.
2θ/degrees
15
20
25
30
35
40
45
(a)
(b)
(c)
(d)
(020)
(011)
(120)
(101)
(111)
(200)
(031)
(131)
(211)
(140)
(012)
(221)
(112)
(321)
* Fe2P
♦ Li3PO4
• Li4P2O7

FIGURE 3

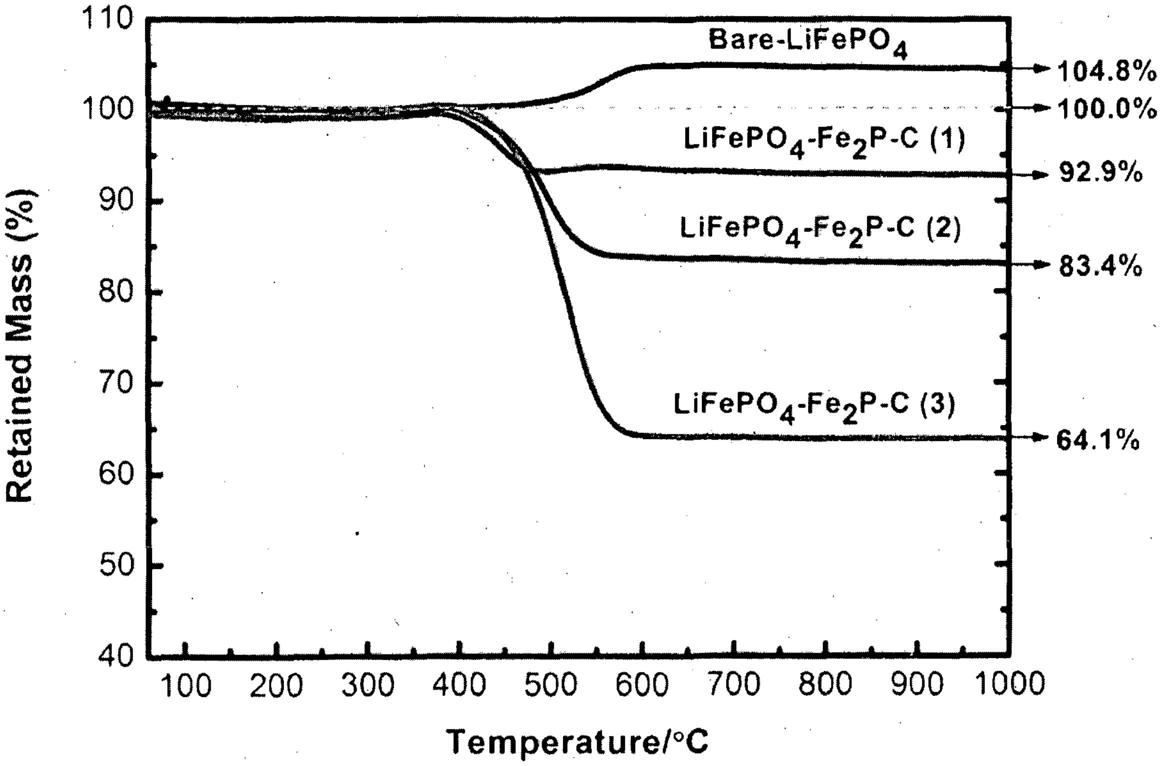
110
100
90
80
70
60
50
40
Retained Mass (%)
100
200
300
400
500
600
700
800
900
1000
Temperature/°C
Bare-LiFePO4
104.8%
100.0%
LiFePO4-Fe2P-C (1)
92.9%
LiFePO4-Fe2P-C (2)
83.4%
LiFePO4-Fe2P-C (3)
64.1%

FIGURE 4

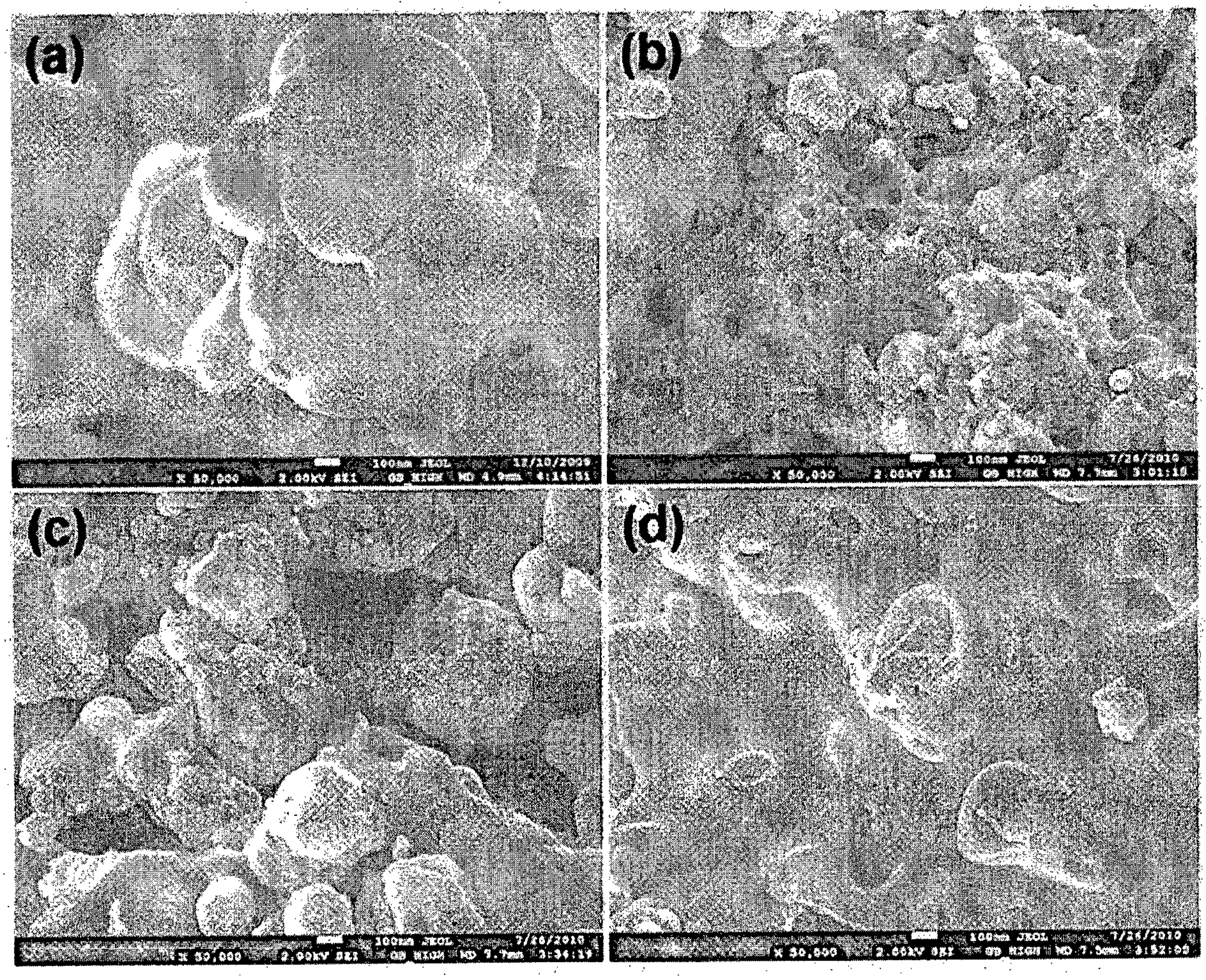
(a)
(b)
(c)
(d)
100nm JEOL 12/10/2009
X 50,000 2.00kV SEI GB HIGH WD 4.9mm 4:14:31
100nm JEOL 7/26/2010
X 50,000 2.00kV SEI GB HIGH WD 7.7mm 3:01:18
100nm JEOL 7/26/2010
X 50,000 2.00kV SEI GB HIGH WD 7.7mm 3:34:19
100nm JEOL 7/26/2010
X 50,000 2.00kV SEI GB HIGH WD 7.5mm 3:52:09

FIGURE 5

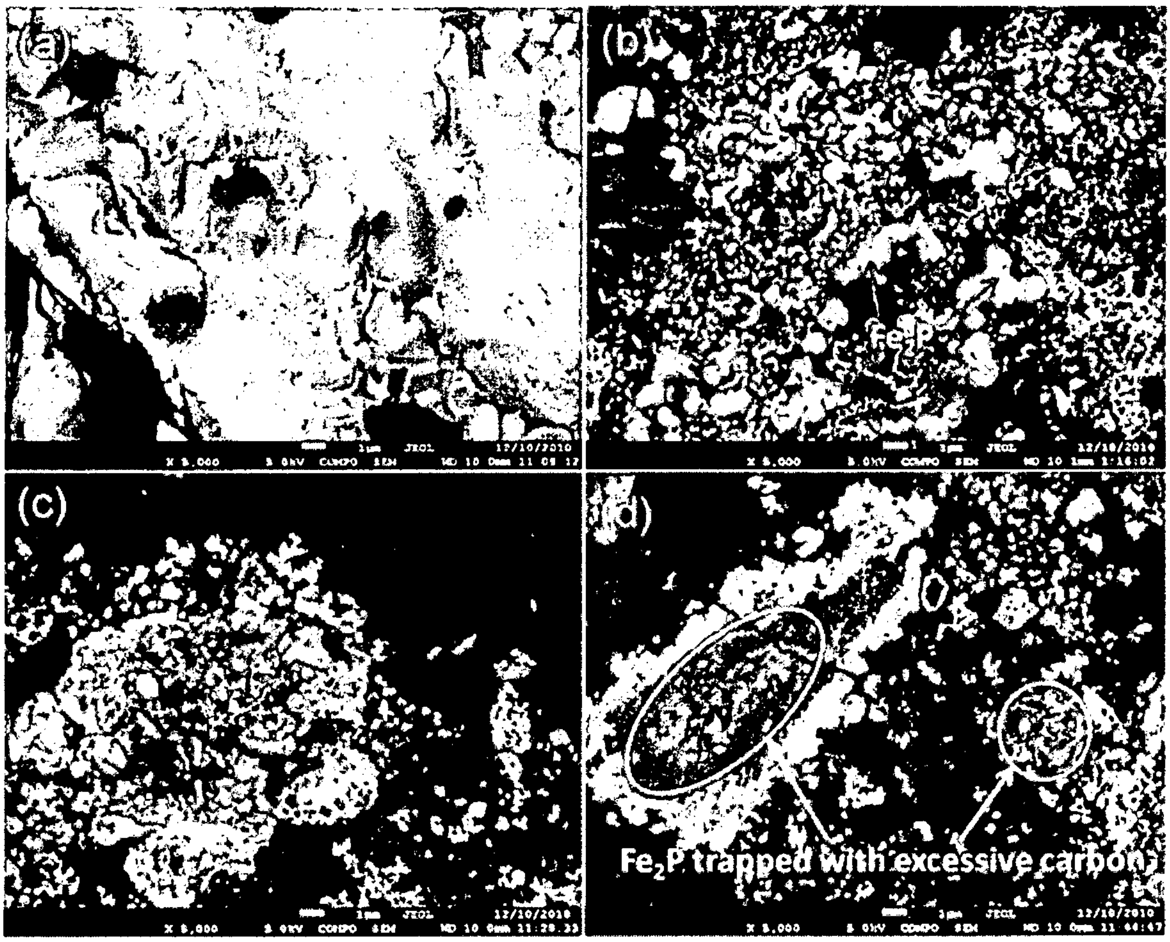
(a)
(b)
Fe_2P
(c)
(d)
Fe_2P trapped with excessive carbon
1μm
JEOL
12/10/2010

FIGURE 6

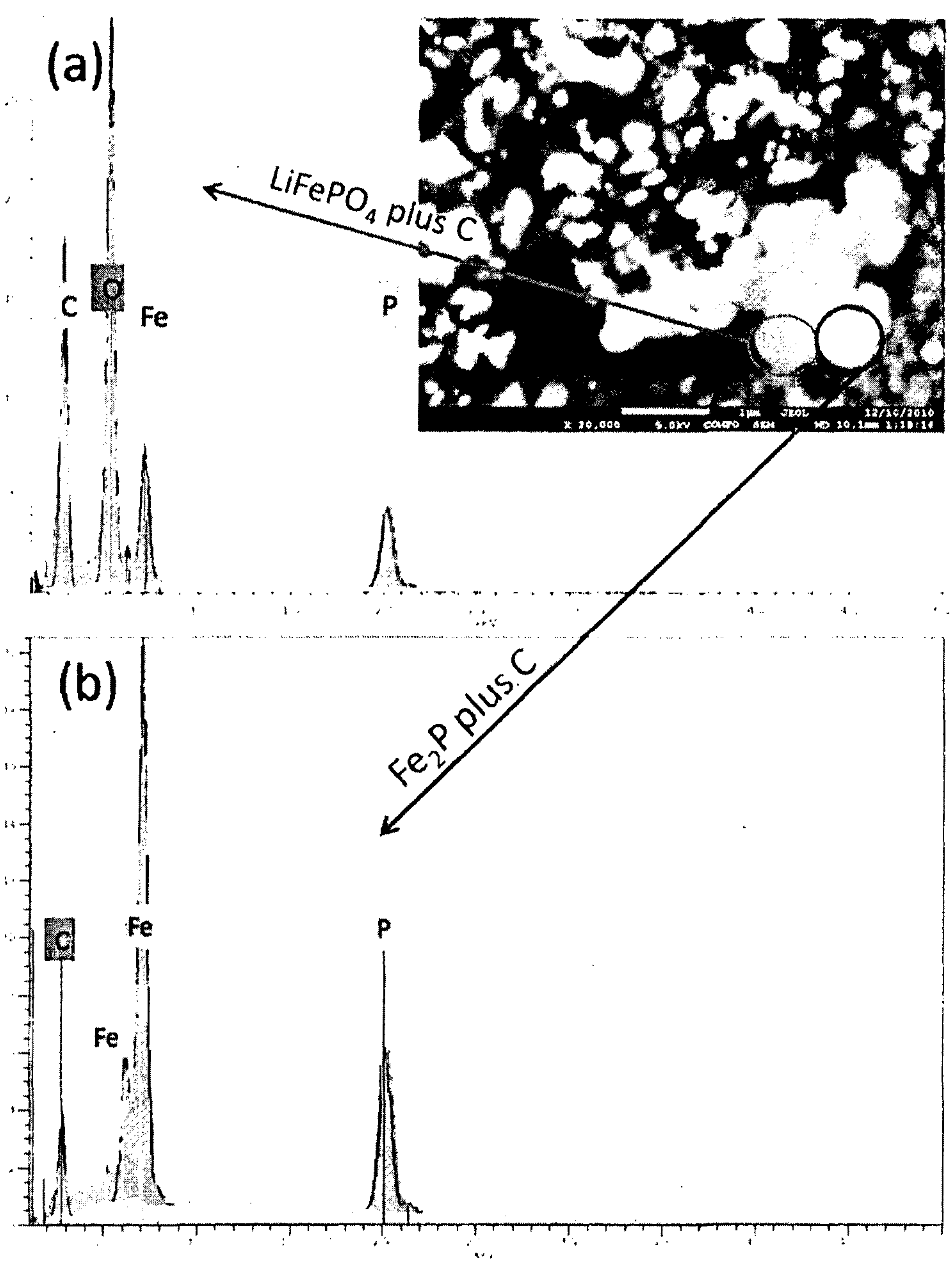
(a)
C
O
Fe
P
LiFePO$_4$ plus C
1μm JEOL 12/10/2010
X 20,000 5.0kV COMPO SEM WD 10.1mm 1:18:14
Fe$_2$P plus C
(b)
C
Fe
Fe
P

FIGURE 7

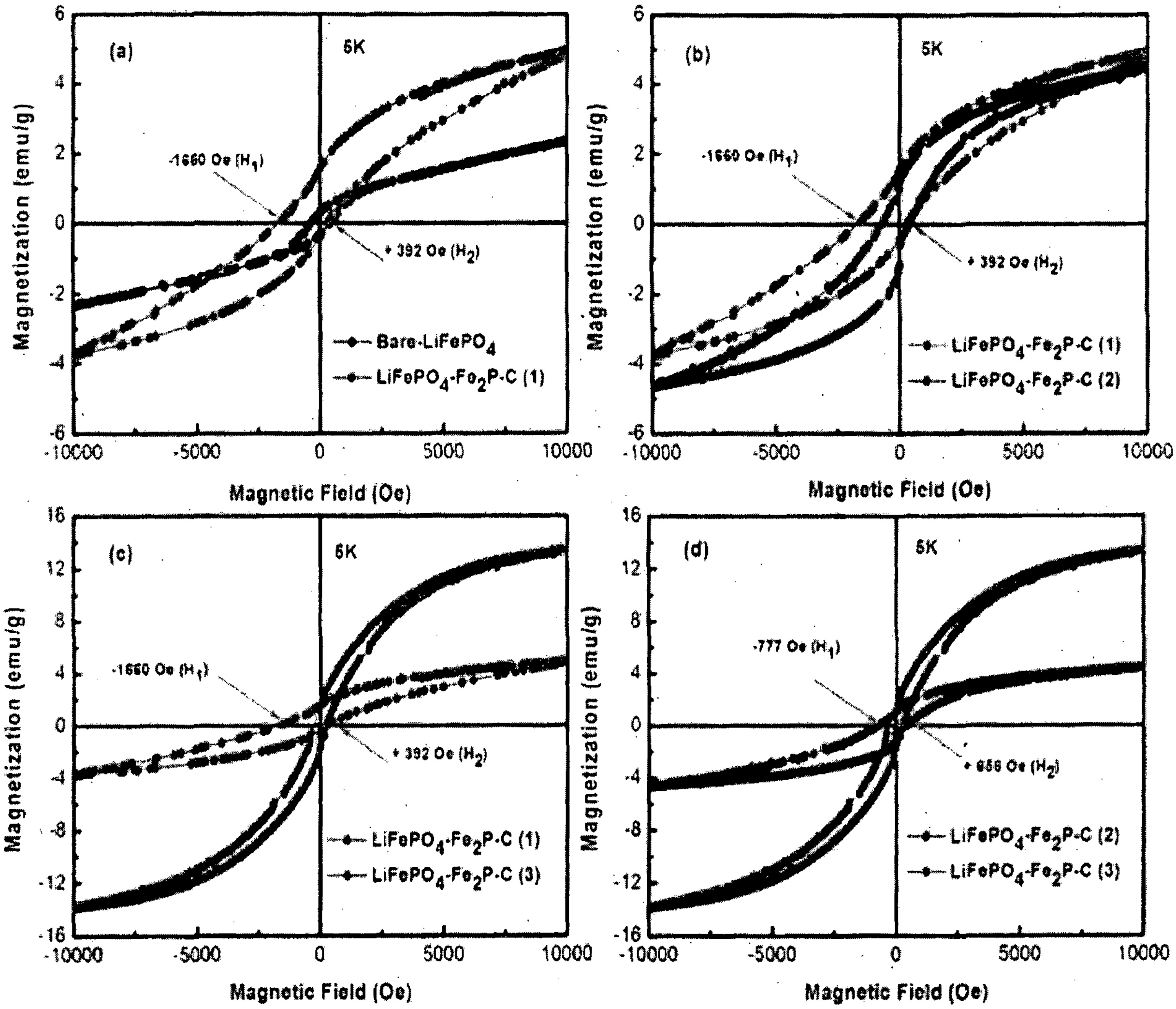
(a)
5K
-1660 Oe (H_1)
+ 392 Oe (H_2)
Bare-LiFePO$_4$
LiFePO$_4$-Fe$_2$P-C (1)
(b)
5K
-1660 Oe (H_1)
+ 392 Oe (H_2)
LiFePO$_4$-Fe$_2$P-C (1)
LiFePO$_4$-Fe$_2$P-C (2)
(c)
5K
-1660 Oe (H_1)
+ 392 Oe (H_2)
LiFePO$_4$-Fe$_2$P-C (1)
LiFePO$_4$-Fe$_2$P-C (3)
(d)
5K
-777 Oe (H_1)
+ 656 Oe (H_2)
LiFePO$_4$-Fe$_2$P-C (2)
LiFePO$_4$-Fe$_2$P-C (3)
Magnetization (emu/g)
Magnetic Field (Oe)
6
4
2
0
-2
-4
-6
16
12
8
4
0
-4
-8
-12
-16
-10000
-5000
0
5000
10000

FIGURE 8

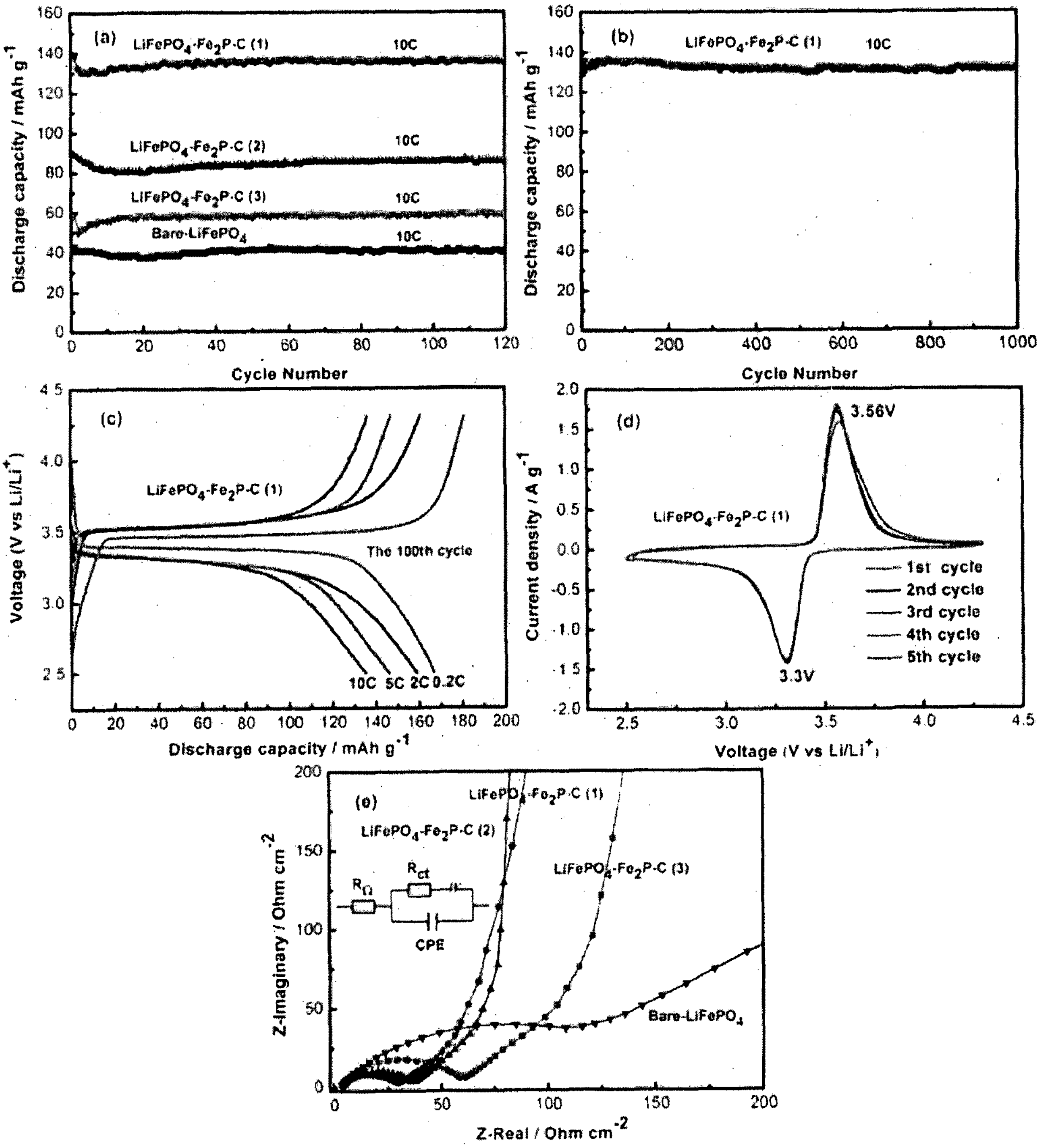
(a)
LiFePO$_4$-Fe$_2$P-C (1) 10C
LiFePO$_4$-Fe$_2$P-C (2) 10C
LiFePO$_4$-Fe$_2$P-C (3) 10C
Bare-LiFePO$_4$ 10C
Discharge capacity / mAh g^{-1}
0 20 40 60 80 100 120 140 160
0 20 40 60 80 100 120
Cycle Number
(b)
LiFePO$_4$-Fe$_2$P-C (1) 10C
Discharge capacity / mAh g^{-1}
0 20 40 60 80 100 120 140 160
0 200 400 600 800 1000
Cycle Number
(c)
LiFePO$_4$-Fe$_2$P-C (1)
The 100th cycle
10C 5C 2C 0.2C
Voltage (V vs Li/Li$^+$)
2.5 3.0 3.5 4.0 4.5
0 20 40 60 80 100 120 140 160 180 200
Discharge capacity / mAh g^{-1}
(d)
3.56V
3.3V
LiFePO$_4$-Fe$_2$P-C (1)
1st cycle
2nd cycle
3rd cycle
4th cycle
5th cycle
Current density / A g^{-1}
-2.0 -1.5 -1.0 -0.5 0.0 0.5 1.0 1.5 2.0
2.5 3.0 3.5 4.0 4.5
Voltage (V vs Li/Li$^+$)
(e)
LiFePO$_4$-Fe$_2$P-C (1)
LiFePO$_4$-Fe$_2$P-C (2)
LiFePO$_4$-Fe$_2$P-C (3)
Bare-LiFePO$_4$
R$_\Omega$
R$_{ct}$
CPE
Z-Imaginary / Ohm cm^{-2}
0 50 100 150 200
0 50 100 150 200
Z-Real / Ohm cm^{-2}

FIGURE 9

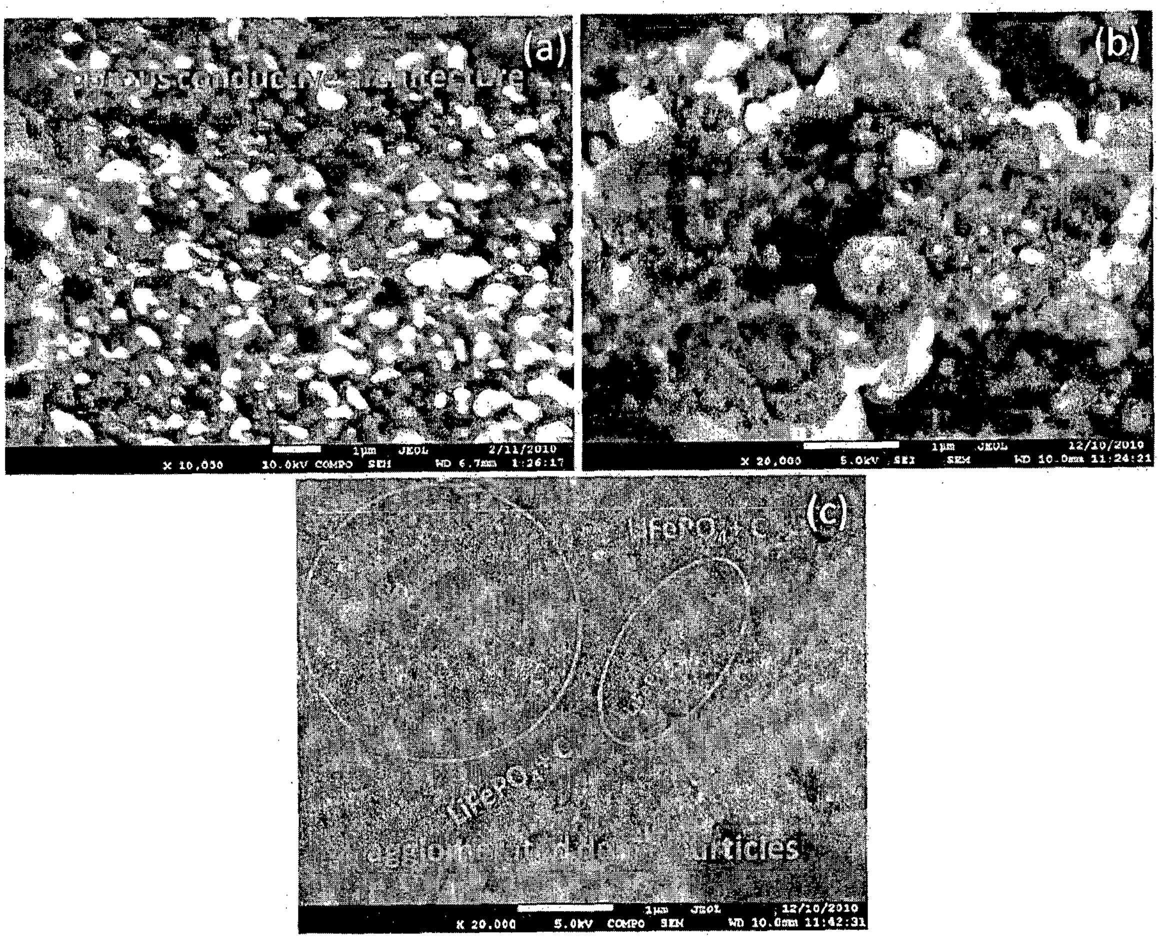
(a)
porous conductive architecture
1µm JEOL 2/11/2010
X 10,030 10.0kV COMPO SEM WD 6.7mm 1:26:17
(b)
1µm JEOL 12/10/2010
X 20,000 5.0kV SEI SEM WD 10.0mm 11:24:21
(c)
LiFePO4+C
LiFePO4+C
agglomerated [illegible] particles
1µm JEOL 12/10/2010
X 20,000 5.0kV COMPO SEM WD 10.0mm 11:42:31

FIGURE 10

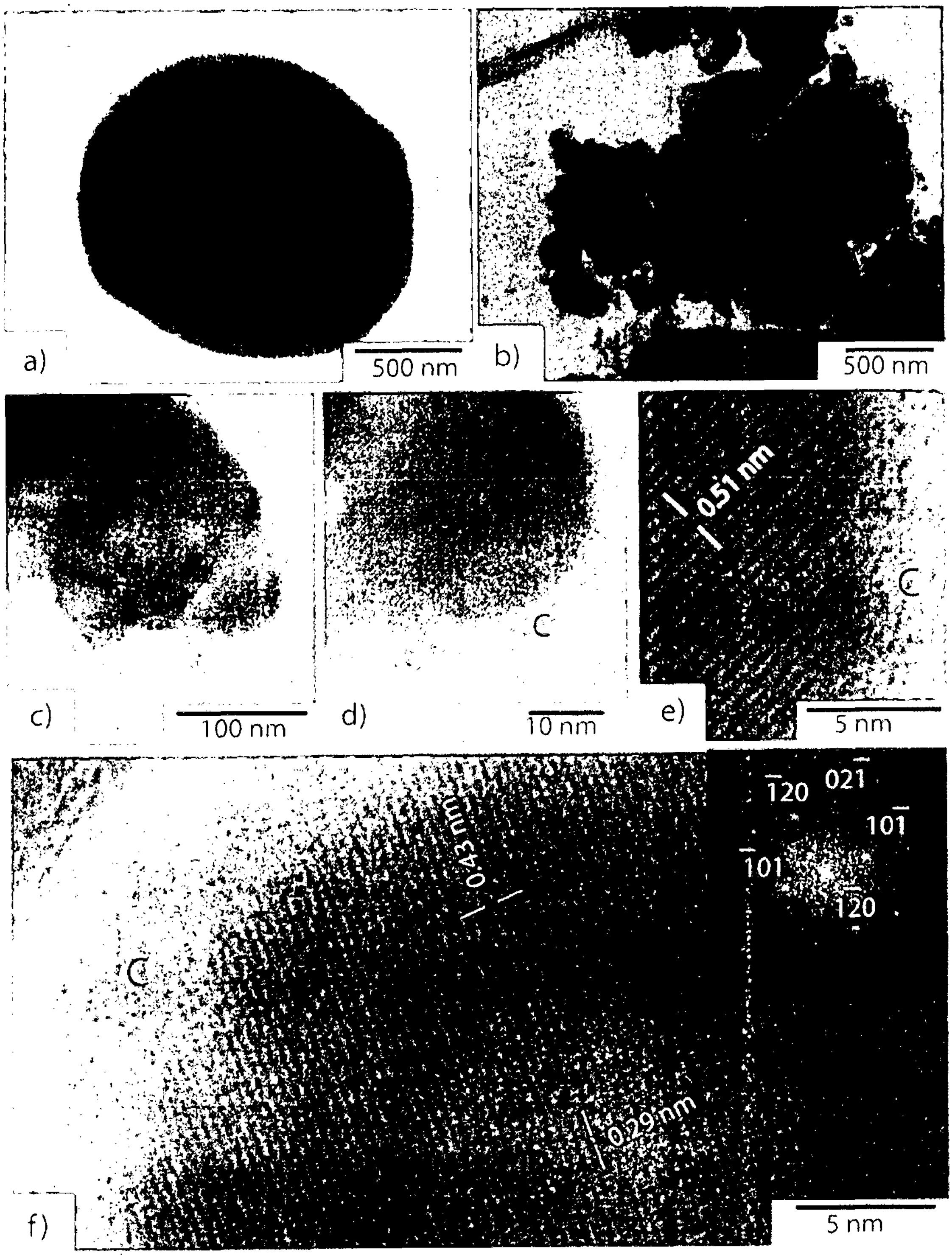
a)
500 nm
b)
500 nm
c)
100 nm
d)
C
10 nm
e)
0.51 nm
C
5 nm
f)
C
0.43 nm
0.29 nm
$\bar{1}20$
$02\bar{1}$
$10\bar{1}$
$\bar{1}01$
$1\bar{2}0$
5 nm

INTERNATIONAL SEARCH REPORT

International application No.
PCT/AU2012/000529

A. CLASSIFICATION OF SUBJECT MATTER

Int. Cl.

C01B 25/26 (2006.01) ***H01M 4/06*** (2006.01) ***H01M 4/38*** (2006.01)
C01B 25/45 (2006.01) ***H01M 4/12*** (2006.01) ***H01M 6/02*** (2006.01)
H01M 4/02 (2006.01) ***H01M 4/36*** (2006.01)

According to International Patent Classification (IPC) or to both national classification and IPC

B. FIELDS SEARCHED

Minimum documentation searched (classification system followed by classification symbols)

Documentation searched other than minimum documentation to the extent that such documents are included in the fields searched

Electronic data base consulted during the international search (name of data base and, where practicable, search terms used)

EPODOC, WPI, CAPLUS, GOOGLE keywords for (Invention 1) lithium, iron, phosphate, milling/grinding and (Invention 2) $LiFePO_4$ and Fe_2P

C. DOCUMENTS CONSIDERED TO BE RELEVANT

Category*	Citation of document, with indication, where appropriate, of the relevant passages	Relevant to claim No.
X	US 2010/0163790 A1 (CEDER et. al.) 1 July 2010 Paragraphs 0044-0072, Examples.	1-28
X	XU et. al., "Synthesis and effect of forming Fe_2P phase on the physics and electrochemical properties of $LiFePO_4$/C materials," *Journal of Power Sources*, No. 160 (2006) pages 570–576. Page 571: "2. Experimental" and "3. Results and Discussion."	1-28
X	US 2009/0035204 A1 (XU et. al.) 5 February 2009 Detailed Description, paragraphs 0034, 0039-0042, 0076, Embodiments.	1-28

☒ Further documents are listed in the continuation of Box C ☒ See patent family annex

* Special categories of cited documents:

"A"	document defining the general state of the art which is not considered to be of particular relevance
"E"	earlier application or patent but published on or after the international filing date
"L"	document which may throw doubts on priority claim(s) or which is cited to establish the publication date of another citation or other special reason (as specified)
"O"	document referring to an oral disclosure, use, exhibition or other means
"P"	document published prior to the international filing date but later than the priority date claimed
"T"	later document published after the international filing date or priority date and not in conflict with the application but cited to understand the principle or theory underlying the invention
"X"	document of particular relevance; the claimed invention cannot be considered novel or cannot be considered to involve an inventive step when the document is taken alone
"Y"	document of particular relevance; the claimed invention cannot be considered to involve an inventive step when the document is combined with one or more other such documents, such combination being obvious to a person skilled in the art
"&"	document member of the same patent family

Date of the actual completion of the international search 30 May 2012	Date of mailing of the international search report 31 May 2012
Name and mailing address of the ISA/AU AUSTRALIAN PATENT OFFICE PO BOX 200, WODEN ACT 2606, AUSTRALIA E-mail address: pct@ipaustralia.gov.au Facsimile No. +61 2 6283 7999	Authorized officer **G. J. BROXAM** AUSTRALIAN PATENT OFFICE (ISO 9001 Quality Certified Service) Telephone No : +61 2 6283 2435

C (Continuation). DOCUMENTS CONSIDERED TO BE RELEVANT

Category*	Citation of document, with indication, where appropriate, of the relevant passages	Relevant to claim No.
X	CN 101339991 A (UNIV. SOUTH CHINA SCI. & ENG. et. al.) 7 January 2009; See Examples. & Derwent Online Abstracts Accession No. 2009-E26290.	1-28
X	DROZD, et. al., "Synthesis, electrochemical properties, and characterization of $LiFePO_4/C$ composite by a two-source method," *Journal of Alloys and Compounds*, Vol. 487 (2009) 58–63. See "2. Experimental" and "3. Results and Discussion."	1-7, 11-13, 15-28
A	PARK, et. al., "The Origin of the Residual Carbon in $LiFePO_4$ Synthesized by Wet Milling," *Bulletin of the Korean Chemical Society*, Vol. 32, No. 2 (20 February 2011), pages 536-540.	
T	RAHMAN et. al., "$LiFePO_4$–Fe_2P–C composite cathode: An environmentally friendly promising electrode material for lithium-ion battery, " *Journal of Power Sources*, No. 206 (25 January 2012), pages 259– 266. Entire document is relevant.	1-32

Box No. II Observations where certain claims were found unsearchable (Continuation of item 2 of first sheet)

This international search report has not been established in respect of certain claims under Article 17(2)(a) for the following reasons:

1. ☐ Claims Nos.:
because they relate to subject matter not required to be searched by this Authority, namely:

2. ☐ Claims Nos.:
because they relate to parts of the international application that do not comply with the prescribed requirements to such an extent that no meaningful international search can be carried out, specifically:

3. ☐ Claims Nos.:
because they are dependent claims and are not drafted in accordance with the second and third sentences of Rule 6.4(a)

Box No. III Observations where unity of invention is lacking (Continuation of item 3 of first sheet)

This International Searching Authority found multiple inventions in this international application, as follows:

See additional sheet.

1. ☐ As all required additional search fees were timely paid by the applicant, this international search report covers all searchable claims.
2. ☒ As all searchable claims could be searched without effort justifying additional fees, this Authority did not invite payment of additional fees.
3. ☐ As only some of the required additional search fees were timely paid by the applicant, this international search report covers only those claims for which fees were paid, specifically claims Nos.:

4. ☐ No required additional search fees were timely paid by the applicant. Consequently, this international search report is restricted to the invention first mentioned in the claims; it is covered by claims Nos.:

Remark on Protest

☐ The additional search fees were accompanied by the applicant's protest and, where applicable, the payment of a protest fee.

☐ The additional search fees were accompanied by the applicant's protest but the applicable protest fee was not paid within the time limit specified in the invitation.

☐ No protest accompanied the payment of additional search fees.

Supplemental Box
(To be used when the space in any of Boxes I to IV is not sufficient)

Continuation of Box No III (Unity of Invention):

This International Application does not comply with the requirements of unity of invention because it does not relate to one invention or to a group of inventions so linked as to form a single general inventive concept.

This Authority has found that there are different inventions based on the following features that separate the claims into distinct groups:

- Claims 1-28. The feature of methods of making lithium composite materials characterised by the defined method steps is specific to this group of claims.
- Claims 29-32. The feature of lithium based composite materials including clusters of olivine phase $LiFePO_4$ and clusters of Fe_2P in close proximity with an interspersed carbon phase is specific to this group of claims.

PCT Rule 13.2, first sentence, states that unity of invention is only fulfilled when there is a technical relationship among the claimed inventions involving one or more of the same or corresponding special technical features. PCT Rule 13.2, second sentence, defines a special technical feature as a feature which makes a contribution over the prior art.

When there is no special technical feature common to all the claimed inventions there is no unity of invention.

In the above groups of claims, the identified features may have the potential to make a contribution over the prior art but are not common to all the claimed inventions and therefore cannot provide the required technical relationship. The only feature common to both sets of claims is the presence of a known material, a lithium-based composite.

Furthermore, as discussed in the Search Opinion, there is convincing evidence that by following the method steps of claim 1, materials other than that of claim 29 may be formed.

Therefore there is no special technical feature common to all the claimed inventions and the requirements for unity of invention are consequently not satisfied *a priori*.

This Annex lists the known "A" publication level patent family members relating to the patent documents cited in the above-mentioned international search report. The Australian Patent Office is in no way liable for these particulars which are merely given for the purpose of information.

Patent Document Cited in Search Report		Patent Family Member					
US	2010163790	CA	2676250	CN	101682029	EP	2111659
		JP	2010517240	WO	2008091707		
US	2009035204	CN	101357756	CN	101407318	EP	2142473
		JP	2010530123	KR	20090131680	WO	2009015565
CN	101339991	NONE					

Due to data integration issues this family listing may not include 10 digit Australian applications filed since May 2001.

END OF ANNEX